

Integrated Cytogenetic Map of Chromosome Arm 4S of *A. thaliana*: Structural Organization of Heterochromatic Knob and Centromere Region

Paul F. Fransz,^{*,†,‡,§} Susan Armstrong,^{*}
J. Hans de Jong,[†] Laurence D. Parnell,[‡]
Cees van Drunen,[§] Caroline Dean,^{||} Pim Zabel,[†]
Ton Bisseling,[†] and Gareth H. Jones^{*}

^{*}School of Biological Sciences
University of Birmingham
Birmingham
United Kingdom

[†]Department of Plant Sciences
Wageningen University
Wageningen
The Netherlands

[‡]Cold Spring Harbor Laboratory
Cold Spring Harbor, New York 11724

[§]E. C. Slater Institute
University of Amsterdam
Amsterdam
The Netherlands

^{||}Department of Molecular Genetics
John Innes Centre
Colney, Norwich NR4 7UH
United Kingdom

Summary

We have constructed an integrated cytogenetic map of chromosome arm 4S of *Arabidopsis thaliana*. The map shows the detailed positions of various multicopy and unique sequences relative to euchromatin and heterochromatin segments. A quantitative analysis of the map positions at subsequent meiotic stages revealed a striking pattern of spatial and temporal variation in chromatin condensation for euchromatin and heterochromatin. For example, the centromere region consists of three domains with distinguishable structural, molecular, and functional properties. We also characterized a conspicuous heterochromatic knob of approximately 700 kb that accommodates a tandem repeat and several dispersed pericentromere-specific repeats. Moreover, our data provide evidence for an inversion event that relocated pericentromeric sequences to an interstitial position, resulting in the heterochromatic knob.

Introduction

The structure and the functioning of a eukaryotic chromosome are basically determined by the molecular organization of the DNA sequences, which not only encode for the RNA transcripts but also determine the specificity of the binding sites for chromatin proteins,

including the transcription machinery. Either the organization of the DNA sequences, the sequence itself, or both is responsible for the higher order organization and thus for the main activities of the chromosome: gene expression, DNA replication, and DNA recombination. A prominent characteristic of the eukaryotic chromosome is its organization into heterochromatic and euchromatic regions. The former is associated with transcriptional inactivity, whereas the latter contains potentially active genes. As euchromatin can become heterochromatic under certain conditions, it is clear that the organization of the chromatin plays an important role in proper regulation of gene expression (Henikoff and Matzke, 1997; Gasser et al., 1998). Significant properties of heterochromatin are replication activity during late S phase, suppression of meiotic recombination (Karpen and Allshire, 1997), and involvement in proper segregation of the homologous chromosomes during meiosis (Dernburg et al., 1996; Karpen et al., 1996). To understand the organization of the euchromatic and heterochromatic components of a eukaryotic chromosome, it is necessary to relate the morphological features of the chromosome with the genetic data and the molecular sequence. The resulting integrated map will provide the tools and information to correlate the DNA sequence with the structure and function of the chromosome.

Integration of the chromosome map and the DNA sequence requires a well-developed system for cytogenetic analysis and an extended sequence database. *Arabidopsis thaliana* has proven an excellent cytogenetic system (Ross et al., 1996; Fransz et al., 1998), in particular in exploiting the relatively uncondensed pachytene chromosomes. It is widely recognized as the prime model system for studying the organization of dicotyledonous plant genomes (Meinke et al., 1998). Its small genome size (120 Mbp per haploid genome) and detailed genetical and physical maps have made this model species most attractive for a whole genome approach. We have chosen the short arm of chromosome 4 of *Arabidopsis* to study the structural organization of a chromosome in a higher eukaryote. The entire arm spans about 9.5 Mbp and is covered by a YAC contig (Schmidt et al., 1995, 1996) of which the complete sequence has been recently established (Mayer et al., 1999). Chromosome arm 4S contains specific euchromatic and heterochromatic regions. For example, a heterochromatic knob, hk4S, which has been discovered in the chromosome arm 4S of some ecotypes (Fransz et al., 1998), resembles the heterochromatic knobs as described in maize (McClintock, 1929; Neuffer et al., 1997). This knob provides an excellent opportunity to study cytological features of heterochromatin as well as the relationship between DNA sequence and heterochromatin formation. A 2.1 Mbp sequenced region containing the heterochromatic knob has been analyzed and is presented in the accompanying paper (McCombie et al., 2000 [this issue of *Cell*]). A second conspicuous heterochromatic region is the centromere region. This region represents 6.5% of the length of an average pachytene chromosome and can be subdivided by fluorescence in situ

To whom correspondence should be addressed (e-mail: fransz@ipk-gatersleben.de). Present address: Institute of Plant Genetics and Crop Plant Research (IPK), Corrensstrasse 3, D-06466 Gatersleben, Germany.

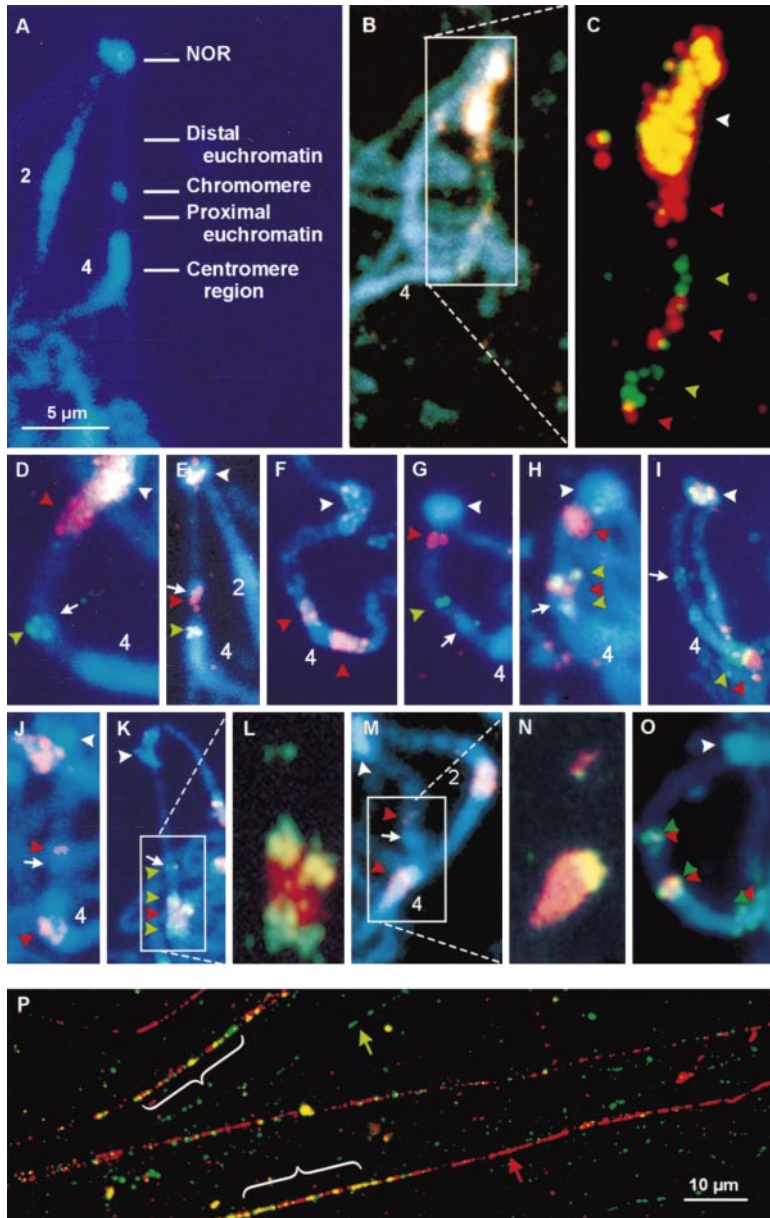


Figure 1. DAPI and FISH Images of Chromosome Arm 4S from Pachytene Cells of WS and Extended DNA Fibers of Columbia

(A) Subdivision of the short arm into five chromosomal subregions. (B and C) From top to bottom: CIC10C8 (red), CIC10H3 (green), CIC4A7 (red), CIC8B1 (green), and CIC7C3 (red); (D) CIC10C8 (red) and CIC8B1 (green); (E) CIC7C3 (red) and 5S rDNA (yellow); (F) CIC5C6 (red); (G) *ANL2* (red) and *GA1* (green); (H) *ANL2* (upper red), *GA1* (upper green), mi233 (red), and mi306 (green); (I) CIC6H11 (red) and CIC11H10 (green); (J) 106B (red); (K and L) pAL1 (red) and F17A20 (green); (M and N) 5S rDNA (yellow), pAL1 (red), and *GA1* (upper red); (O) T1J24 (red) and F10A2 (green). The colored arrowheads indicate the FISH signals on the chromosome. The white arrows indicate the position of the knob. The Arabic numbers indicate the centromere region of the corresponding chromosome. The presence of FISH signals of the NOR (white arrowhead) in (B)–(F) and (I) was due to hybridization with yeast ribosomal DNA sequences.

(P) Fiber-FISH signals of the tandemly repetitive 5S rDNA (red) reveal long continuous stretches (long arrow), whereas those of the dispersed repeat F17A20 (green) are shorter (short arrow). Yellow signals or alternating colors (brackets) denote adjacent and interspersed localization of the two sequences.

hybridization (FISH) into the centromere, containing the 180 bp repeat, and two flanking pericentromeric domains (Fransz et al., 1998).

Cytogenetic and molecular data have so far provided valuable information about the distribution of repetitive sequences along the chromosomes. The fact that only 10% of the *Arabidopsis* genome consists of repeats (Leutweiler et al., 1984), which are mainly present in the heterochromatin regions around the centromere and the nucleolar organizing region (NOR), implies that the euchromatin contains an exceptionally low proportion of repetitive DNA sequences. In conjunction, these developments have stimulated us to create a detailed integrated cytogenetic and molecular map in order to relate the morphological features of the chromosome, e.g., euchromatic and heterochromatic segments, to the underlying DNA sequence. Further, we discuss how the observed cytological and molecular characteristics of

euchromatin and heterochromatin might be related with chromosome functioning.

Results

Construction of a Molecular Cytogenetic Map of Chromosome Arm 4S

As a first step in aligning cloned DNA sequences and chromosomal structures, we applied FISH to midprophase cells, including late zygotene, pachytene, and early diplotene stages, the former and last only when a discernible, fully paired short arm of chromosome 4 was observed. In addition, only cells with uniformly stretched euchromatic and heterochromatic regions and traceable arms were recorded. Based on the structural characteristics of chromosome arm 4S, we defined five regions (Figure 1A): the NOR (I), the distal euchromatic region (II), the heterochromatic knob, hk4S (III), the proximal

Table 1. Cytological and Molecular Distances of Markers in the Short Arm of Chromosome 4

Region	Marker	n	Average relative Distance (%) ^a	Average Absolute Distance (μm) ^b	Molecular Distance (kb) ^c	Corresponding BACs ^e
I	NOR	93	100	9.6	2860	—
II	CIC10C8-d ^d	18	97.6 ± 2.3	9.4	2800	T15P10
	<i>ANL2</i>	18	87.4 ± 4.9	8.4	2640	F15P23
	CIC10H3-d	4	79.8 ± 7.7	8.2	2310	F2N1
	CIC10C8-p	18	76.6 ± 5.3	7.4	2340	F2N1
	CIC10H3-p	4	66.1 ± 12.4	7.3	1850	T2H3
	CIC4A7-d	13	63.8 ± 7.5	6.4	1800	T14P8
	<i>GA1</i>	38	51.4 ± 7.5	4.8	1520	T5J8
	CIC4A7-p	13	46.4 ± 5.7	4.6	1370	F4C21
	CIC8B1-d	17	43.3 ± 5.8	4.3	1290	F9H3
	mi233	9	43.6 ± 4.5	4.2	1160	F9H3
III	knob-d	88	41.6 ± 5.8	3.9	—	—
	CIC7C3-d	33	33.5 ± 4.7	3.1	470	T19B17
	knob-p	88	31.9 ± 4.8	3.1	—	—
IV	mi306	5	32.1 ± 2.8	3.1	400	T26N26
	CIC8B1-p	17	28.4 ± 6.1	2.8	310	T26N26
	CIC7C3-p	33	21.1 ± 3.7	2.0	0	T1J1
V	pericentromere	88	16.5 ± 2.9	1.6	—	—
	5SrRNA-d	38	15.8 ± 2.4	1.5	—	—
	5SrRNA-p	37	6.8 ± 2.6	0.7	—	—
	pAL1-d	14	6.2 ± 2.0	0.6	—	—

^aRelative to centromere.

^bAbsolute distance to centromere in an average sized arm (CEN-NOR = 9.58 μm) based on linear regression analysis.

^cDistance to the most proximal YAC marker (CIC7C3-p) (from Schmidt et al., 1996).

^dSince YAC signals display regions rather than discrete spots, a distal (d) and a proximal (p) site are distinguished.

^eDetermined from the physical map and the BAC tiling path (<http://www.arabidopsis.org/chr4.html>).

euchromatic segment (IV), and the centromere region of the short arm (V). The molecular markers were selected from different regions along the short arm according to the physical map (Schmidt et al., 1996). They include small unique DNA fragments, repetitive DNA sequences, and YAC clones that make up a contig extending from the rDNA locus to the 180 bp repeat of the centromeric region, known as pAL1 (Martinez-Zapater et al., 1986) or AtCon (Heslop-Harrison et al., 1999). Five YACs spanning a region of 2.8 Mbp hybridized to the major part of the short arm, showing a pattern of alternating red and green fluorescent arrays (Figures 1B and 1C). Three of these YACs (CIC10C8, CIC10H3, and CIC4A7) cover the distal euchromatin (region II), YAC clone CIC8B1 colocalized with the knob (region III) (Figure 1D), and CIC7C3 hybridized mainly with the proximal euchromatic region IV and slightly overlapped with the knob (Figure 1E). Two proximal YACs from the short arm, CIC3F1 and CIC3C8, and the YAC clone CIC5C6 in the long arm hybridized to the peripheral domains of the pericentromeric heterochromatin of all chromosomes (Figure 1F). This indicates that these YACs contain several abundant pericentromeric repeat sequences that impede accurate mapping.

We verified the chromosomal position of the YACs in the distal euchromatin with a λ clone containing the homeobox gene *ANL2*, which has been genetically mapped in the region covered by CIC10C8 (Kubo et al., 1999), and a cosmid with the gibberelin gene *GA1* (Sun and Kamiya, 1994) that has been physically and genetically mapped in the region covered by CIC4A7. FISH signals of *ANL2* and *GA1* were found close to the NOR and the knob, respectively, (Figure 1G) thus confirming

the chromosomal position of the euchromatic YACs. To verify the colocalization of YAC clone CIC8B1 with the knob, we used the RFLP markers mi233 and mi306, which are located close to the ends of the YAC clone CIC8B1 (Schmidt et al., 1996). Their FISH signals indeed flanked the knob (Figure 1H). We estimate the molecular size of hk4S to be less than the physical distance (760 kb) between mi233 and mi306.

By measuring the arm length (CEN-NOR distance) and the distance of each marker to the centromere, a cytogenetic map was constructed in two ways. At first, average relative distances were determined by taking the ratio of the distance of each marker relative to the CEN-NOR distance. Secondly, the average absolute distances of all markers were plotted against the arm length in a linear regression analysis resulting in predicted positions of a marker along the chromosome arm. The two methods gave similar map positions (Table 1). From the cytogenetic map, we estimated the molecular position of the pericentromeric heterochromatin border in the short arm. The hybridization signal of clone CIC7C3 was found at 0.4 μm from the heterochromatic segment (Table 1). Based on the condensation degree of region IV (see below), this distance corresponds with approximately 160 kb. In conjunction with the sequence database (McCombie et al., 2000), we expect the border of the pericentromeric heterochromatin at the proximal site of YAC clone CIC3F1. FISH signals of YACs CIC11H10 (380 kb) and CIC6H11 (460 kb) that were physically mapped in contig 2 and contig 3, respectively (Schmidt et al., 1996), revealed the pericentromeric border in the long arm adjacent to CIC11H10 (Figure 1I). The presented cytogenetic map thus shows a perfect

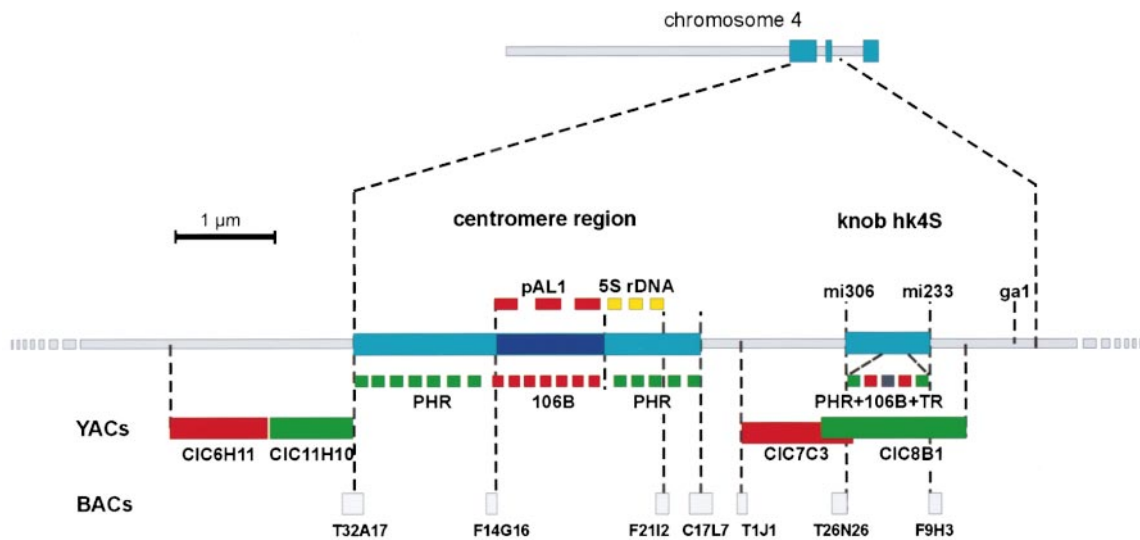


Figure 2. Molecular Cytogenetic Map of the Centromere Region of *Arabidopsis* Chromosome 4

Heterochromatic segments are depicted as blue boxes, of which the dark blue box forms the centromere. Euchromatic domains are shown in gray. The colored boxes above and below the centromere region represent tandem and dispersed repeats. The alignment with BACs is based on the sequence map (Mayer et al., 1999). PHR, pericentromeric heterochromatin repeats. TR, 1950 bp tandem repeat of the knob hk4S.

alignment with the physical map up to the pericentromeric heterochromatin. Repeats present within this heterochromatic segment, however, hamper the mapping of unique sequences. So far, all tested proximal YACs showed hybridization signals in the distal parts of the pericentromeric heterochromatin and not the central region.

Structural Organization of the (Peri)Centromeric Heterochromatin

The (peri)centromeric heterochromatin in DAPI-stained pachytene chromosomes is visible as a bright fluorescent region around a central less fluorescent domain (Ross et al., 1996). Previous FISH studies with repeats from the centromere region on interphase nuclei and metaphase chromosomes (Maluszynska and Heslop-Harrison, 1991; Brandes et al., 1997) were not able to resolve the adjacent different heterochromatic domains. We analyzed the molecular organization of the (peri)centromeric heterochromatin in pachytene chromosomes using a number of DNA clones that have been physically and genetically mapped close to the centromere (Schmidt et al., 1996; Thompson et al., 1996; Copenhaver et al., 1998; Round et al., 1997; <http://nucleus.cshl.org/protarab>). The 180 bp tandem repeat, pAL1, and the 106B repeat, which is a diverged copy of the LTR of the *Athila* retrotransposon (Pelissier et al., 1995, 1996), occupy the central domain in all chromosomes (Figures 1J–1L). This region represents the functional centromere (Fransz et al., 1998; see also Figure 4). No hybridization signals were observed in the flanking pericentromeric domains. In contrast, the BAC clones T1J24 and F10A2, which have been physically mapped very close to the 180 bp centromere repeat of chromosome 4, contain repeats that hybridize predominantly to the flanking domains (Figure 1O). Like the proximal YACs shown above (Figure 1F), the same hybridization pattern of these BACs was

found on all chromosomes, suggesting all pericentromeric regions to contain the same repeats. This is verified with hybridization signals on chromosome 4 of the BAC clone F17A20 (Figures 1K and 1JL) that has been physically mapped close to the centromere of chromosome 1 (Mozo et al., 1998). Sequence analysis of the BACs T1J24 and F10A2 revealed that they consist for 20% to 30% of transposon elements, of which *Athila* is the most prominent. The 5S rDNA repeat, previously mapped in the long arm of chromosome 4 close to pAL1 (Schmidt et al., 1996), appears to hybridize in the pericentromeric heterochromatin of the short arm adjacent to the central pAL1 domain (Figures 1M and 1N). A study of the molecular organization of pericentromeric repeats with extended DNA fibers revealed long tandem arrays of 5S rDNA genes (Figure 1P) up to several hundreds of kilobases (not shown). A similar long tandemly arrayed pattern has been found for pAL1 (Jackson et al., 1998). In contrast, the repeats from the pericentromeric BACs display a dispersed pattern of hybridization signals, alternated with short stretches, sometimes colocalizing with the 5S rDNA arrays (Figure 1P). These data show that the centromeric and pericentromeric repeats occupy separate domains (Figure 2). In all chromosomes the centromere contains the tandemly repetitive 180 bp repeat, interrupted with the 106B repeat and possibly other repetitive elements, while the pericentromere contains dispersed repeats consisting of transposon elements. In addition, the pericentromere of chromosome 4 also contains the tandemly arrayed 5S rDNA.

Chromatin (De)Condensation Patterns Reveal Spatial and Temporal Differences between and within Eu- and Heterochromatin Segments

By aligning the cytogenetic map with the physical molecular map, we are now able to quantitate the condensation degree in kb/μm of heterochromatin and euchromatin along the chromosome arm. The heterochromatic

Table 2. Condensation Characteristics of Subchromosomal Regions in the Short Arm of Chromosome 4

Region	Flanking Markers		Cytol. Size (μm)	Molec. Size (kb) ^a	Condensation Degree (kb/ μm) ^b	Decondensation Factor ^c
I	telomere	NOR	1.65 ^d	3700 ^e	2240	ND
Ila	CIC10C8-d	CIC10C8-p	2.0	460	230	1.7
Ilb	CIC10C8-p	CIC4A7-d	1.0	540	540	2.8
Ilc	CIC4A7-d	mi233	2.4	640	270	1.2
III	mi233/chrom-d	mi306/chrom-p	1.1	760	700	1.1
IV	mi306	CIC7C3-p	1.2	400	330	1.4
II-IV	CIC10C8-d	CIC7C3-p	7.4	2860	390	1.5
V	CEN	pericentromere-d	1.6	ND	ND	1.3

^aData from Schmidt et al. (1996) and McCombie et al. (2000).

^bIn an average 9.6 μm arm.

^cExpressed as the increase in cytological size from early/mid pachytene (CEN-NOR = 7.5 μm) to early diplotene (CEN-NOR = 11.4 μm).

^dData from Franz et al. (1998).

^eData from Copenhagen and Pikaard (1996).

knob, hk4S, (700 kb/ μm) and especially the NOR (2.2 Mb/ μm) are highly condensed compared to the euchromatin region (330 kb/ μm). This is well illustrated by

the larger area that hybridizes to the YAC CIC10C8 (510 kb) compared to CIC8B1 (990 kb) in Figure 1D. Although the euchromatin region is uniformly stained by DAPI, a significant variation in chromatin condensation was observed within the distal euchromatin. A subdivision of region II into smaller segments revealed a strong variation in condensation degree within the euchromatic segment. For example, the regions Ila (230 kb/ μm) and Ilb (540 kb/ μm) differ by a factor 2.5 (Table 2). Interestingly, the less condensed area around *ANL2* (170 kb/ μm) corresponds with a relatively hot spot for recombination (Schmidt et al., 1995).

The variation in chromatin condensation between the different regions was monitored not only spatially but also temporally, since the arm length varied between 6 and 17 μm depending on the meiotic substage. Midprophase I cells were determined by the degree of synapsis, the rate of chromosome clustering, and the distribution of the organelles as described previously (Ross et al., 1996). Early pachytene chromosomes were among the smallest and early diplotene chromosomes among the longest, while late zygotene and late pachytene chromosomes were found in the medium-sized class (Figure 3A). This suggests that chromosomes condense up to early pachytene and starts to extend from mid-pachytene.

To investigate if this (de)condensation pattern involves the entire arm or only a few specific regions, we calculated for each region the decondensation factor (DF), which is the increase in size from early pachytene to early diplotene (Table 2). It appeared that the distal euchromatin (DF = 1.7), especially region Ilb (DF = 2.8), is strongly subjected to decondensation and, thus, more flexible, while the heterochromatic knob hardly shows decondensation. The phenomenon of differential chromatin condensation along euchromatin and heterochromatin is clearly visualized in Figure 3B, showing the positions of the YAC clone CIC7C3 and 5S rDNA in conjunction with the heterochromatic knob and the pericentromere heterochromatin at subsequent meiotic stages. A small proximal euchromatin region is observed at early pachytene, whereas during zygotene, late pachytene, and early diplotene this region is significantly larger, especially compared to the heterochromatic knob and the pericentromere, represented by the 5S rDNA signal. The relatively unchanged size of the pericentromere compared to the centromere indicates that

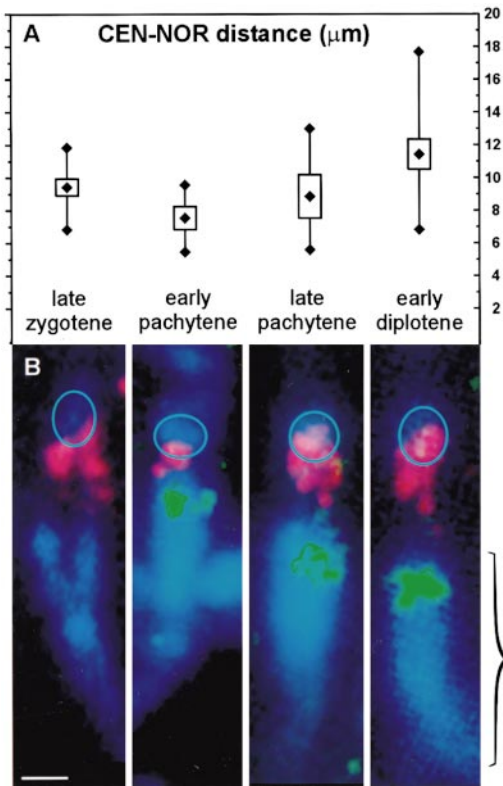


Figure 3. Length Variation of Chromosome Arm 4S and Differential Chromatin Condensation around CEN4 at Subsequent Prophase I Stages

(A) Box-Whisker diagram with mean, SD, and $1.96 \times \text{SD}$ values of the CEN-NOR distance. Measurements were carried out on fully paired short arms of chromosome 4. Toward pachytene the chromosome condenses, whereas after pachytene decondensation takes place. (B) FISH images of subsequent prophase I stages of WS hybridized with CIC7C3 (red) and 5S rDNA (green). The size of the proximal euchromatin (distance between CIC7C3 and 5S rDNA) varies, whereas the knob size (blue circle) remains the same. Also, note the variation of the centromere region (bracket) compared to the 5S rDNA signal. The zygotene cells were not hybridized with 5S rDNA. Bar = 1 μm .

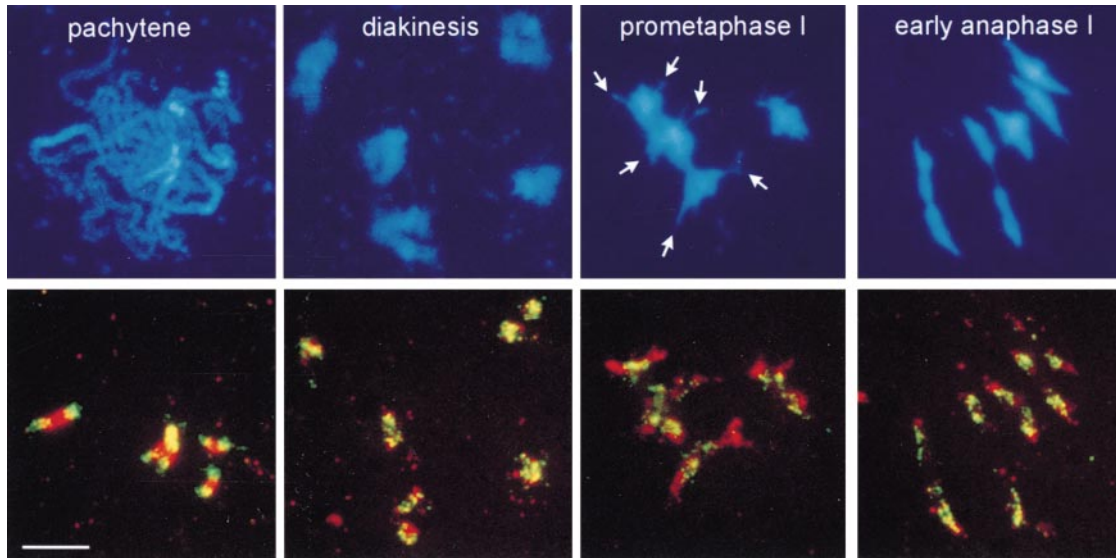


Figure 4. FISH Images of Subsequent Meiotic Stages of *Ler* with (Peri)Centromeric Repeats

The centromere and the pericentromere, visualized with 106B (red) and F17A20 (green), respectively, condense and colocalize at diakinesis. At prometaphase I a reversion of the domains has taken place. Red hybridization signals of the centromere repeats cover a large area of the bivalent, including DNA-positive protrusions (arrow). At early anaphase I the red signals are at the most pole-ward positions of the bivalent, indicating that centromeres are pulled to opposite poles. Note the contrast in size between the red and the green signals at subsequent stages. Bar = 5 μ m.

these heterochromatic domains have different chromatin condensation properties. This is confirmed by the decondensation factor of the centromere and the pericentromere (1.7 and 1.1, respectively). The difference in condensation patterns of centromere and pericentromere, respectively, is also visible during later stages of meiosis (Figure 4). After the pachytene stage, the homologs separate but are physically connected at the chiasmata and condense toward diakinesis. As a result, the centromere and the pericentromere colocalize. Each bivalent has reached a maximum state of condensation at the phase of repulsion, during prometaphase I. However, the hybridization signals (red) of the centromere repeats cover a large area of the bivalent, including DAPI-positive protrusions, while the pericentromere repeat signals (green) are only observed in the central area. We did not find such extended hybridization signals with any other DNA clone. This indicates that the centromere has obviously decondensed during prometaphase I, in contrast to the rest of the bivalent. Finally, establishment of the kinetochore activity is reached at metaphase I. At this time the homologs are pulled to opposite poles with the centromeres in leading position as shown by the most pole-ward directed projections of the centromere repeats. During these meiotic stages, the pericentromere shows no or little changes in (de)condensation, thus underlining the different structural properties of centromere and pericentromere.

Cytological and Molecular Characteristics of the Heterochromatic Knob, hk4S

The heterochromatic knob, hk4S, is observed only in the ecotypes WS and Col (Figure 5A) and is absent from *Ler* (Figure 5B) and C24 (Figure 5C). It resembles the knobs in maize (McClintock, 1929; Neuffer et al., 1997)

but is less pronounced and not visible during premeiotic interphase (data not shown). During leptotene chromatin thickenings in the two nonaligned homologous chromosomes distal from the CIC7C3 region indicate the formation of the heterochromatic knob. Since the knobs of the two homologs may differ in size, chromatin condensation in the homologs does not necessarily take place simultaneously. Furthermore, the molecular markers mi233 and mi306 mark the edges of the knob throughout midprophase I irrespective of the condensation degree of the chromosome arm. This implies that the molecular size of the hk4S does not change significantly during this period.

FISH analysis revealed the presence of centromeric and pericentromeric repeats in the knob but not in the euchromatin (Figures 1J, 1K, and 1O), indicating these repeats to be a major difference between the heterochromatic knob and the euchromatic segments. In the accompanying paper, McCombie et al. (2000) confirm the presence of abundant repetitive elements in the heterochromatic knob, of which *Athila* is the most prominent. Moreover, their sequence analysis of a 2.1 Mbp contiguous region, including the knob region, shows that the knob is characterized by a low density of expressed genes. We examined the repetitive nature of the repeats in all sequenced BACs by a dot-plot analysis and discovered a tandemly arranged repeat in the knob region (BAC clone T5H22) with a basic unit of 1950 bp that contains inverted and direct repeat elements. In contrast, all other repeats in the euchromatin and the knob show a dispersed distribution. The 1950 kb repeat element is related to the *Tam/Spm* family of transposon elements (McCombie et al., 2000) and is reiterated 22 times spanning in total 44 kb. FISH analysis with a 417 bp fragment of the tandem repeat revealed hybridization

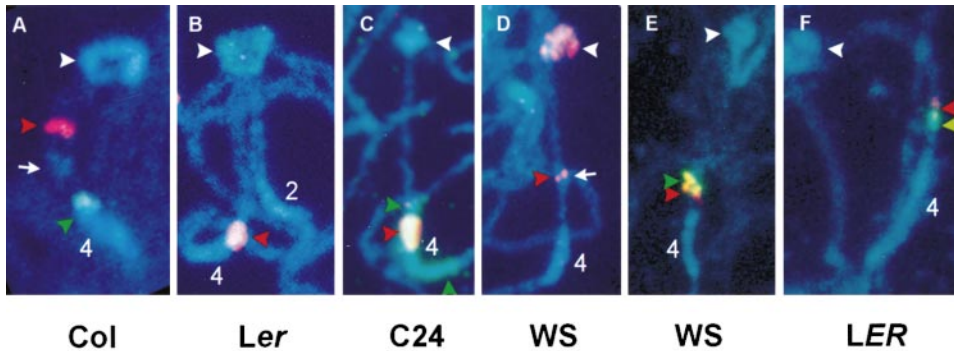


Figure 5. FISH Images Showing Polymorphism around the Knob Region between *Arabidopsis* Ecotypes

(A) Col, hybridized with GA1 (red) and 5S rDNA (green).

(B) Ler, hybridized with 5S rDNA (red), lacks the knob.

(C) C24, hybridized with 5S rDNA (yellow) and F17A20 (green) lacks the knob and knob repeats.

(D) WS, hybridized with a 417 bp DNA fragment of the tandem repeat from the heterochromatic knob.

(E and F) WS and LER, hybridized with the BACs T1J1 (red) and T4B21 (green), show a reversed position of the hybridization signals.

The colored arrowheads indicate the FISH signals on the chromosome. The numbers indicate the centromere region of the corresponding chromosome. White arrow, knob; white arrowhead, NOR.

signals in the distal half of the knob and in the NOR segment (Figure 5D), while faint hybridization signals were found in the pericentromeric heterochromatin.

The polymorphism of the hk4S knob between WS and Col on the one hand and Ler, LER, and C24 on the other suggests a chromosomal rearrangement in this area. This idea is reinforced by the absence of the pericentromeric repeats at the hk4S position in the knob-less ecotypes and the fact that the RFLP marker mi233, which flanks the knob at the distal end, is absent from ecotype Ler (Liu et al., 1996). In order to obtain more information about the putative rearrangement, we hybridized two contiguous BACs, T1J1 and T1B21, that have been mapped proximal from the knob region of ecotype Col (McCombie et al., 2000). We found the BAC signals in WS at the same position and orientation (Figure 5E) as described in the sequence map of Col. Surprisingly, in the ecotype LER the BACs T1J1 and T4B21 were at the same position but showed a reversed orientation (Figure 5F), indicating an inversion event. We speculate that the inversion has brought pericentromeric heterochromatin sequences to an interstitial position, thus creating an interstitial heterochromatic knob.

Discussion

Cytogenetic Reconstruction of Chromosome Arm 4S

The data presented in this paper show a detailed molecular cytogenetic analysis of a complete chromosome arm, resulting in an integrated cytogenetic and physical map of chromosome arm 4S, including the molecular markers and eu- and heterochromatic segments. In *Arabidopsis* the majority of repetitive elements is restricted to the heterochromatic segments around the centromere and at the NORs. This allowed the differential paint of the major part of chromosome arm 4S, which demonstrates the molecular cytogenetic potency of the model plant *Arabidopsis*. The differential paint is considered a significant achievement in cytogenetics, especially in plants, since individual chromosome painting has been

unsuccessful due to the distribution of repetitive sequences all over the genome (Fuchs et al., 1996). Only in the case of addition lines, which contain a single alien chromosome, has chromosome painting been established by applying alien total genomic DNA as probe (Heslop-Harrison et al., 1990). Another advantage of *Arabidopsis* cytogenetics is the extended pachytene chromosomes, which have proven preeminently appropriate for high resolution mapping studies. The average length of a midprophase I chromosome after Carnoy fixation is 66 μm (Franz et al., 1998). In comparison, chromosome mapping in the model systems yeast ($n = 16$) and *C. elegans* ($n = 6$) are performed on synaptonemal complexes (SCs) of pachytene cells, which span on average 1.8 μm (Loidl et al., 1991) and 6.8 μm (Goldstein, 1986), respectively. Although FISH has been applied successfully to yeast SCs (Scherthan et al., 1992) an explicit differentiation between heterochromatin and euchromatin domains has not been made. The detailed mapping of heterochromatic regions in *Arabidopsis* will be a valuable tool to study its structure, in particular the organization of repeats and the sequences at the boundaries that together are essential for its functioning in epigenetic mechanisms of gene regulation as shown in *Drosophila* and yeast (Wallrath, 1998).

Centromere and Pericentromere Are Structurally and Functionally Different Regions

The centromere region in *Arabidopsis* pachytene chromosomes is confined to an intensely stained DAPI-positive region and shows a sharp transition to the euchromatin. In chromosome 4 it spans 4 μm , which corresponds to 6.5% of the entire pachytene chromosome length (Franz et al., 1998). Based on a 700 kb/ μm condensation degree for heterochromatin, we estimate the size of the entire centromere region at approximately 3 Mbp, of which the centromere contains about 1 Mbp. This is consistent with size estimates of the 180 bp repeat in other publications (Round et al., 1997; Jackson et al., 1998). A close physical linkage between the 180 bp tandem repeat and several middle repetitive sequences

has been reported by molecular studies (Pelissier et al., 1996) and FISH analysis on interphase nuclei (Brandes et al., 1997). However, they were not able to discriminate between centromere and pericentromere. This FISH study has clearly distinguished the centromere from the two flanking pericentromeric domains on the basis of morphological appearance, condensation properties, and molecular composition. The three domains, which together form the centromere region (Figure 2), are distinct during meiosis, especially in pachytene cells, whereas in somatic cells they colocalize during G1 (P. F. F. et al., unpublished data). The centromere is largely composed of abundant tandemly arranged 180 bp repeats and dispersed repeats, such as 106B, whereas the pericentromere contains mainly transposon elements, a.o. Athila. The pericentromere of chromosome 4 has a predicted gene density of less than 1 per 100 kb (Mayer et al., 1999) and accommodates DNA elements that can be transcriptionally activated (Steimer et al., personal communication). In addition, the short arm contains the 5S rDNA genes, which are among the most highly expressed genes. It differs from the adjacent euchromatin in morphological appearance, gene density, and the presence of abundant dispersed repeats.

The structural differences between the centromere and the pericentromere are also reflected in the spatial position and the condensation properties of these segments in subsequent meiotic stages. From pachytene to metaphase I, these heterochromatic domains change position in the bivalent structure. After pachytene the chromosomes have to resolve the crossovers and prepare for a proper disjunction of the homologs. Condensation takes place over the entire chromosome, in particular in the euchromatin and the centromere. However, during prometaphase I the centromere shows a remarkable decondensation, covering a relatively large area of the bivalent surface. It is possible that this spatial reorganization facilitates the spindle microtubules to attach to the bivalent, thus ensuring a proper disjunction of the homologs. This would strengthen the idea that the centromere might be regulated by an epigenetic mechanism, in which the higher order structure of the centromeric heterochromatin contributes to kinetochore assembly (Karpen and Allshire, 1997). In mouse oocytes it has been shown that during prometaphase I microtubules attach to the surface of the chromosomes but not yet to the kinetochore (Brunet et al., 1999). Stable kinetochore microtubule interactions are established at the end of congression near the equatorial plane, allowing the final alignment of the bivalents and subsequent movement of the homologs to opposite poles. If a similar sequence of events would occur in *Arabidopsis*, then the decondensed centromere would likely be involved in the attachment of the microtubules along the surface of the bivalent.

The Heterochromatic Knob, hk4S, Originates from the Pericentromeric Outer Domain

Heterochromatic knobs have been associated with low transcriptional and recombination activity. Indeed, the complete sequence of a 2.1 Mbp region around the heterochromatin knob hk4S reveals a low gene density in the knob, while the number and variation of DNA

repeats is high (McCombie et al., 2000). In addition, alignment with the genetic (ColXLer) map (Lister and Dean, 1993) demonstrates that the condensed knob region corresponds with a cold spot of recombination. Due to the low frequency in the region spanning the centromere and the hk4S locus, this segment has been assigned to the genetically defined centromere (Copenhaver et al., 1999). However, in these crosses it is more likely that suppression of recombination is the result of knob heterozygosity between Col and Ler, rather than the heterochromatic component alone, since the knob and the repetitive sequences are absent from the ecotype Ler (Fransz et al., 1998). FISH analysis with the BACs T1J1 and T4B21 on pachytene chromosomes of Ler and WS revealed an inversion in the short arm 4S. Although these two BACs span only 140 kb, we propose that the inversion includes the proximal euchromatin and the heterochromatic knob. Preliminary FISH data with several ecotypes and BACs around the hk4S locus (P. F. F. et al., unpublished data) indeed suggest the region covered by the BACs T5L23 to T32N4 to be involved in the inversion. We postulate that the heterochromatic knob, hk4S, originates from an inversion event that moved DNA sequences from the pericentromere to a more distal position in the euchromatin. Additional evidence for a pericentromeric origin of hk4S comes from the molecular and cytological similarities between the knob and the pericentromere. Both regions are heterochromatic, have a high condensation degree, a comparable decondensation factor, a low gene density, and the same DNA repeats. The pericentromeric domain may therefore be considered as a heterochromatic knob or, according to the description of Lima-de-Faria (1983), a chromomere.

The question arises as to whether the repetitive nature or the sequence or both is responsible for the heterochromatic nature of the knob. Considering the fact that the tandem repeat occupies a disproportionately small region (44 kb), compared to the size of the knob (~700 kb), we suggest that the organization of a tandem repeat with flanking dispersed repeats is a prerequisite for the heterochromatic nature of the knob. A similar combined organization of tandem repeats and dispersed retrotransposable elements has been described for heterochromatic knobs in maize (Ananiev et al., 1998). However, some basic differences exist between the *Arabidopsis* knob and the maize knobs. Unlike most maize knobs, the tandem repeat region of hk4S is continuous and not interrupted by other repeats. The knob hk4S contains several pericentromeric repeats, whereas maize knobs show less homology with pericentromeric repeats. Furthermore, the hk4S knob is small and has a proximal position close to the pericentromeric heterochromatin. Finally, no neocentric activity of hk4S has been observed. These data and the fact that the knob is so far only detected in the ecotypes WS and Col suggest that hk4S may have been formed recently. Considering the similarity between the cytogenetic map of WS and the sequence map of Col versus the differences with Ler and C24, our data would place WS close to Col in the phylogenetic tree of ecotypes. Indeed a close relationship between Col and WS has been suggested on the basis of DNA polymorphism (Hardtke et al., 1996).

In conclusion, *Arabidopsis* is an eukaryotic organism

with a well-defined and characteristic organization of heterochromatin and euchromatin segments. The presented integrated cytogenetic map of the short arm of chromosome 4 permits to correlate heterochromatin with specific DNA elements and provides an excellent experimental system to investigate which DNA sequences are responsible for heterochromatin formation and which function as a chromatin domain boundary element. This will help to elucidate the role of heterochromatin in epigenetic regulation of gene expression.

Experimental Procedures

Plant Material

Inflorescences were harvested from ecotypes Wassilekija (WS), Columbia (Col), C24, and Landsberg *erecta* (laboratory strain *Ler* as well as parental strain *LER*). Seeds from *LER*, obtained from Dr. Rédei, were shown to be isogenic to *Ler* by AFLP analysis (C. Alonso-Blanco and A.J.M. Peeters, unpublished data). Flower buds were fixed in Carnoy's fluid (ethanol/acetic acid 3:1) and chromosome spreads prepared according to Ross et al. (1996). Extended DNA fibers were prepared from isolated leaf nuclei of ecotype Columbia according to Fransz et al. (1996).

Probes

The following DNA clones were used: a 700 bp *SacI*-*XbaI* fragment of the 25S ribosomal gene of *Petunia* (van Blokland et al., 1994); pCT4.2, a 0.5 kb *Sall* fragment containing the 5S ribosomal gene of *A. thaliana* (Campbell et al., 1992); 106B, a 0.4 kb *EcoRI* fragment (EMBL accession number X93611), which is a diverged copy of the LTR region of the *Athila* retrotransposon (Thompson et al., 1996); pAL1, containing a 180 bp repeat sequence (Martinez-Zapater et al., 1986); CIC10C8, CIC10H3, CIC4A7, CIC8B1, CIC7C3, CIC5C6, CIC6H11, and CIC11H10 are YAC clones from the CIC library (Creusot et al., 1996); F17A20 and F10A2 are BAC clones from the IGF library (Mozo et al., 1998); T1J1, T1J24, and T1B21 are BAC clones from the TAMU library (Choi et al., 1995); GA1 is a cosmid that maps to the *GA1* locus on chromosome arm 4S (Sun and Kamiya, 1994); ANL2 is a λ clone containing the *ANL2* homeobox gene (Kubo et al., 1999); mi233 and mi306 are RFLP markers (Liu et al., 1996). A 427 bp DNA fragment of the tandem repeat from the knob hk4S was amplified by PCR using the primers 5'-GCTTAAGATCAA TAATGGT-3' and 5'-TAAATTAAGAAAATAAGTTT-3', which were constructed from the tandem repeat in the BAC clone T5H22. All DNA clones and PCR products were labeled with either biotin-dUTP, digoxigenin-dUTP, or a combination of both, using a nick translation kit (Boehringer Mannheim).

Fluorescence In Situ Hybridization

Fluorescence in situ hybridization was carried out using the methods described by Fransz et al. (1998). Chromosome preparations were baked at 60°C for 30 min. After incubating with RNase (10 μ g/ml in 2 \times SSC), the slides were rinsed in 2 \times SSC buffer for 2 \times 5 min and in PBS (10 mM sodium phosphate [pH 7.0] 143 mM NaCl) for 2 \times 5 min and subsequently fixed in 1% (v/v) paraformaldehyde in PBS for 10 min, rinsed in PBS for 2 \times 5 min, dehydrated through an ethanol series (70%, 90%, and 100%, each 2 min), and air dried. To each slide 20 μ l of denaturation buffer (70% formamide, 2 \times SSC, 50 mM sodium phosphate [pH 7.0]) was added and denatured on a hot block of 75°C for 2 min. After removal of the coverslips the slides were washed in ice-cold 70% ethanol for 2 min, dehydrated in an ethanol series (70%, 90%, and 100%, each 2 min) at room temperature, and air dried.

The hybridization mix contained 100 ng probe in 50% formamide, 2 \times SSC, 50 mM sodium phosphate (pH 7.0), and 10% dextran sulfate. The slides were incubated with 20 μ l denatured hybridization mix in a moist chamber at 37°C for 18 hr in general and for 2 days when YAC DNA was used as probe. Posthybridization washes were performed in 50% formamide, 2 \times SSC (pH 7.0) for 3 \times 5 min at 42°C followed by 2 \times SSC at room temperature for 3 \times 5 min. Double

fluorescence detection of the probes was performed according to Fransz et al. (1998).

Microscopy

Hybridization signals were examined with a Nikon Labophot 2 or a Zeiss Axioplan. Selected images were directly photographed on a 400 Provia Fujichrome film using single (for DAPI), double (for FITC and Texas red), and triple (for DAPI, FITC, and Texas red) fluorescence filter blocks. Images were further processed to enhance brightness and contrast with Adobe Photoshop computer software.

Measurements

The arm length is defined here as the distance between the centromere and NOR. Since the NORs of chromosomes 2 and 4 are often fused to one heterochromatic region, the telomeric end of the short arm can not be distinguished. Therefore, we used the transition of NOR to distal euchromatin as one of the bench markers for the short arm. The other bench marker is formed by the middle of the pericentromeric heterochromatin, which colocalizes with a less fluorescent area and is considered in most cytogenetic studies as the centromere. This is confirmed in this study by the hybridization signals of the 180 bp pAL1 tandem repeat. The midpoint of each fluorescent signal is taken to measure the position of the marker. In the case of hybridization signals from YACs and tandem repeats, the borders of the fluorescent region were used as individual markers indicated by d (distal) and p (proximal).

Acknowledgments

We thank Drs. M. Koornneef, C. Alonso-Blanco, and C. Heyting for helpful discussions and critical reading of the manuscript, Drs. M. Stammers, R. Schmidt, and T. Peeters for providing material and data of the DNA clones, and Mrs. P. Zhang for her contribution in preparing the data of Figures 2E and 2H. The project was supported by the European Community (grant numbers CHRX-CT94-0511 and PL960443).

Received October 26, 1999; revised January 10, 2000.

References

- Ananiev, E.V., Phillips, R.L., and Rines, H.W. (1998). Complex structure of knob DNA on maize chromosome 9: retrotransposon invasion into heterochromatin. *Genetics* 149, 2025-2037.
- Brandes, A., Thompson, H., Dean, C., and Heslop-Harrison, J.S. (1997). Multiple repetitive DNA sequences in the paracentromeric regions of *Arabidopsis thaliana* L. *Chromosome Res.* 5, 238-246.
- Brunet, S., Maria, A.S., Guillaud, P., Dujardin, D., Kubiak, J.Z., and Maro, B. (1999). Kinetochores are not involved in the formation of the first meiotic spindle in mouse oocytes, but control the exit from the first meiotic M phase. *J. Cell Biol.* 146, 1-11.
- Campbell, B.R., Song, Y., Posch, T.E., Cullis, C.A., and Town, C.D. (1992). Sequence and organization of 5S ribosomal RNA-encoding genes of *Arabidopsis*. *Gene* 112, 225-228.
- Choi, S., Creelman, R.A., Mullet, J.E., and Wing, R. (1995). Construction and characterization of a bacterial artificial chromosome library of *Arabidopsis thaliana*. *Plant Mol. Biol. Rep.* 13, 124-128.
- Copenhaver, G., and Pikaard, C.S. (1996). RFLP and physical mapping with an rDNA-specific endonuclease reveals that the nucleolus organizing regions of *Arabidopsis thaliana* adjoin the telomeres on chromosomes 2 and 4. *Plant J.* 9, 259-272.
- Copenhaver, G.P., Browne, W.E., and Preuss, D. (1998). Assaying genome-wide recombination and centromere functions with *Arabidopsis* tetrads. *Proc. Natl. Acad. Sci. USA* 95, 247-252.
- Copenhaver, G.P., Nickel, K., Kuromori, T., Benito, M.I., Kaul, S., Lin, X., Bevan, M., Murphy, G., Harris, B., Parnell, L.D., et al. (1999). Genetic definition and sequence analysis of *Arabidopsis* centromeres. *Science* 286, 2468-2474.
- Creusot, F., Fouilloux, E., Dron, M., Lafleurie, J., Picard, G., Billault, A., Le Paslier, D., Cohen, D., Chaboué, M.E., Durr, A., et al. (1996).

- The CIC library: a large insert YAC library for genome mapping in *Arabidopsis thaliana*. *Plant J.* **8**, 763–770.
- Dernburg, A.F., Sedat, J.W., and Hawley, R.S. (1996). Direct evidence of a role for heterochromatin in meiotic chromosome segregation. *Cell* **86**, 135–146.
- Fransz, P.F., Alonso-Blanco, C., Liharska, T.B., Peeters, A.J.M., Zabel, P., and de Jong, J.H. (1996). High resolution physical mapping in *Arabidopsis thaliana* and tomato by fluorescence in situ hybridization to extended DNA fibers. *Plant J.* **9**, 421–430.
- Fransz, P., Armstrong, S., Alonso-Blanco, C., Fischer, T.C., Torres-Ruiz, R.A., and Jones, G.H. (1998). Cytogenetics for the model system *Arabidopsis thaliana*. *Plant J.* **13**, 867–876.
- Fuchs, J., Houben, A., Brandes, A., and Schubert, I. (1996). Chromosome 'painting' in plants—a feasible technique? *Chromosoma* **104**, 315–320.
- Gasser, S.M., Paro, R., Stewart, F., and Aasland, R. (1998). The genetics of epigenetics. *Cell. Mol. Life Sci.* **54**, 1–5.
- Goldstein, P. (1986). The synaptonemal complex of *Ceanorhabditis elegans*: pachytene karyotype analysis of hermaphrodites from the recessive *him-5* and *him-7* mutants. *J. Cell Sci.* **82**, 119–127.
- Hardtke, C.S., Muller, J., and Berleth, T. (1996). Genetic similarity among *Arabidopsis thaliana* ecotypes estimated by DNA sequence comparison. *Plant Mol. Biol.* **322**, 915–922.
- Henikoff, S., and Matzke, M. (1997). Exploring and explaining epigenetic effects. *Trends Genet.* **13**, 293–295.
- Heslop-Harrison, J.S., Leitch, E.R., Schwarzacher, T., and Ananthawat-Jonsson, K. (1990). Detection and characterization of 1B/1R translocation in hexaploid wheat. *Hereditas* **65**, 385–392.
- Heslop-Harrison, J.S., Murata, M., Ogura, Y., Schwarzacher, T., and Motoyoshi, F. (1999). Polymorphism and genomic organization of repetitive DNA from centromeric regions of *Arabidopsis* chromosomes. *Plant Cell* **11**, 31–42.
- Jackson, S.A., Wang, M.I., Goodman, H.M., and Jiang, J. (1998). Application of fiber-FISH in physical mapping of *Arabidopsis thaliana*. *Genome* **41**, 566–572.
- Karpen, G.H., and Allshire, R.C. (1997). The case for epigenetic effects on centromere identity and function. *Trends Genet.* **13**, 489–496.
- Karpen, G.H., Le, M.-H., and Le, H. (1996). Centric heterochromatin and the efficiency of achiasmate disjunction in *Drosophila* female meiosis. *Science* **273**, 118–122.
- Kubo, H., Peeters, A.J.M., Aarts, M.G.M., Pereira, A., and Koornneef, M. (1999). *Anthocyanless2*, a homeobox gene affecting anthocyanin distribution and root development in *Arabidopsis*. *Plant Cell* **11**, 1217–1226.
- Leutweiler, L.S., Hough-Evans, B.R., and Meyerowitz, E.M. (1984). The DNA of *Arabidopsis thaliana*. *Mol. Gen. Genet.* **194**, 15–23.
- Lima-de-Faria, A. (1983). Molecular evolution and organization of the chromosome (Amsterdam, NY: Elsevier).
- Lister, C., and Dean, C. (1993). Recombinant inbred lines for mapping RFLP and phenotypic markers in *Arabidopsis thaliana*. *Plant J.* **4**, 745–750.
- Liu, Y.-G., Mitsukawa, N., Lister, C., Dean, C., and Whittier, R.F. (1996). Isolation and mapping of a new set of 129 RFLP markers in *Arabidopsis thaliana* using recombinant inbred lines. *Plant J.* **10**, 733–736.
- Loidl, J., Nairz, K., and Klein, F. (1991). Meiotic chromosome synapsis in a haploid yeast. *Chromosoma* **100**, 221–228.
- Maluszynska, J., and Heslop-Harrison, J.S. (1991). Localization of tandemly repeated DNA sequences in *Arabidopsis thaliana*. *Plant J.* **1**, 159–166.
- Martinez-Zapater, J.M., Estelle, M.A., and Somerville, C.R. (1986). A highly repeated DNA sequence in *Arabidopsis thaliana*. *Mol. Gen. Genet.* **204**, 417–423.
- Mayer, K., Schüller, C., Wambutt, R., Murphy, G., Volckaert, G., Pohl, T., Dusterhoft, A., Stiekema, W., Entian, K.D., Terryn, N., et al. (1999). Sequence and analysis of chromosome 4 of the plant *Arabidopsis thaliana*. *Nature* **402**, 769–777.
- McClintock, B. (1929). Chromosome morphology in *Zea mays*. *Science* **69**, 629.
- McCombie, W.R., de la Bastide, M., Habermann, K., Parnell, L., Dedhia, N., Gnoj, L., Schutz, K., Huang, E., Spiegel, L., Yordan, C., et al. (2000). The complete sequence of a heterochromatic island from a higher eukaryote. *Cell* **100**, this issue, 377–386.
- Meinke, D.W., Cherry, J.M., Dean, C., Rounsley, S.D., and Koornneef, M. (1998). *Arabidopsis thaliana*: a model plant for genome analysis. *Science* **282**, 679–682.
- Mozo, T., Fischer, S., Meier-Ewert, S., Lehrach, H., and Altmann, T. (1998). Use of the IGF BAC library for physical mapping of the *Arabidopsis thaliana* genome. *Plant J.* **16**, 377–384.
- Neuffer, M.G., Coe, E.H., and Wessler, S.R. (1997). Mutants of Maize, Cytological Map (Plainview, NY: Cold Spring Harbor Laboratory Press), p. 32.
- Pelissier, T., Tutois, S., Deragon, J.M., Tourmente, S., Genestier, S., and Picard, G. (1995). Athila, a new retroelement from *Arabidopsis thaliana*. *Plant Mol. Biol.* **29**, 441–452.
- Pelissier, T., Tutois, S., Tourmente, S., Deragon, J.M., and Picard, G. (1996). DNA regions flanking the major *Arabidopsis thaliana* satellite are principally enriched in Athila retroelement sequences. *Genetica* **97**, 141–151.
- Ross, K., Fransz, P., and Jones, G.H. (1996). A light microscopic atlas of meiosis in *Arabidopsis thaliana*. *Chromosome Res.* **4**, 507–516.
- Round, E.K., Flowers, S.K., and Richards, E.J. (1997). *Arabidopsis thaliana* centromere regions: genetic map positions and repetitive DNA structure. *Genome Res.* **7**, 1045–1053.
- Scherthan, H., Loidl, J., Schuster, T., and Schweizer, D. (1992). Meiotic chromosome condensation and pairing in *Saccharomyces cerevisiae* studied by chromosome painting. *Chromosoma* **101**, 590–595.
- Schmidt, R., West, J., Love, K., Lenehan, Z., Lister, C., Thompson, H., Bouchez, D., and Dean, C. (1995). Physical map and organization of *Arabidopsis thaliana* chromosome 4. *Science* **270**, 480–483.
- Schmidt, R., West, J., Cnops, G., Love, K., Balestrazzi, A., and Dean, C. (1996). Detailed de-scription of four YAC contigs representing 17 Mb of chromosome 4 of *Arabidopsis thaliana* ecotype Columbia. *Plant J.* **9**, 755–765.
- Sun, T.P., and Kamiya, Y. (1994). The *Arabidopsis* *GA1* locus encodes the cyclase ent-kautrene synthetase a of gibberelin biosynthesis. *Plant Cell* **6**, 1509–1518.
- Thompson, H., Schmidt, R., and Dean, C. (1996). Identification and distribution of seven classes of middle repetitive DNA in the *Arabidopsis thaliana* genome. *Nucleic Acids Res.* **24**, 3017–3022.
- van Blokland, R., Van der Geest, N., Mol, J.M.N., and Kooter, J.M. (1994). Transgene-mediated suppression of chalcon synthase expression in *Petunia hybrida* results from an increase in RNA turnover. *Plant J.* **6**, 861–877.
- Wallrath, L.L. (1998). Unfolding the mysteries of heterochromatin. *Curr. Opin. Genet. Dev.* **8**, 147–153.